



Since January 2020 Elsevier has created a COVID-19 resource centre with free information in English and Mandarin on the novel coronavirus COVID-19. The COVID-19 resource centre is hosted on Elsevier Connect, the company's public news and information website.

Elsevier hereby grants permission to make all its COVID-19-related research that is available on the COVID-19 resource centre - including this research content - immediately available in PubMed Central and other publicly funded repositories, such as the WHO COVID database with rights for unrestricted research re-use and analyses in any form or by any means with acknowledgement of the original source. These permissions are granted for free by Elsevier for as long as the COVID-19 resource centre remains active.

In-silico network pharmacology study on *Glycyrrhiza glabra*: Analyzing the immune-boosting phytochemical properties of Siddha medicinal plant against COVID-19

Karthik Sekaran^a, Ashwini Karthik^b, Rinku Polachirakkal Varghese^a,
P. Sathyarajeswaran^c, M.S. Shree Devi^d, R. Siva^a, and
C. George Priya Doss^{a,*}

^aSchool of Biosciences and Technology, Vellore Institute of Technology, Vellore, India

^bDepartment of Biology, Mount Carmel College Autonomous, India

^cSiddha Regional Research Institute, Puducherry, India

^dSiddha Central Research Institute, CCRS, Chennai, India

*Corresponding author. e-mail address: georgepriyadoss@vit.ac.in

Contents

1. Introduction	2
2. Materials and methods	4
2.1 Mining of phytoconstituents and its target	4
2.2 Enrichment and network analysis	5
2.3 Druglikeness and ADMET profiling	6
2.4 Molecular docking	6
2.5 Molecular dynamics simulation	6
3. Results	7
3.1 Phytoconstituents and their target	7
3.2 Gene-set enrichment analysis and network analysis	8
3.3 Druglikeness and ADMET profiling	8
3.4 Molecular docking	12
3.5 Molecular dynamics simulation	14
4. Discussion	17
5. Conclusion	19
CRedit authorship contribution statement	20
Data availability statement	20
Declaration of competing interest	20
Appendix A Supporting information	20
References	20

Abstract

Immunosenescence is a pertinent factor in the mortality rate caused by Severe Acute Respiratory Syndrome Coronavirus 2 (SARS-CoV-2). The changes in the immune system are strongly associated with age and provoke the deterioration of the individual's health. Traditional medical practices in ancient India effectively deal with COVID-19 by boosting natural immunity through medicinal plants. The anti-inflammatory and antiviral properties of *Glycyrrhiza glabra* are potent in fighting against COVID-19 and promote immunity boost against the severity of the infection. Athimadhura Chooranam, a polyherbal formulation containing *Glycyrrhiza glabra* as the main ingredient, is recommended as an antiviral Siddha herb by the Ministry of AYUSH. This paper is intended to identify the phytoconstituents of *Glycyrrhiza glabra* that are actively involved in preventing individuals from COVID-19 transmission. The modulated pathways, enrichment study, and drug-likeness are calculated from the target proteins of the phytoconstituents at the pharmacological activity (Pa) of more than 0.7. Liquiritigenin and Isoliquiritin, the natural compounds in *Glycyrrhiza glabra*, belong to the flavonoid class and exhibit ameliorative effects against COVID-19. The latter compound displays a higher protein interaction to a maximum of six, out of which *HMOX1*, *PLAU*, and *PGR* are top-hub genes. ADMET screening further confirms the significance of the abovementioned components containing better drug-likeness. The molecular docking and molecular dynamics method identified liquiritigenin as a possible lead molecule capable of inhibiting the activity of the major protease protein of SARS-CoV-2. The findings emphasize the importance of *in silico* network pharmacological assessments in delivering cost-effective, time-bound clinical drugs.

Abbreviations

ADMET	Absorption Distribution Metabolism Excretion and Toxicity
ChEBI	Chemical Entities of Biological Interest
KEGG	Kyoto Encyclopedia of Genes and Genomes
MPP	Main Protease Proteins
MDS	Molecular Dynamics Simulation
RMSD	Root-Mean-Square Deviation
RMSF	Root-Mean-Square Fluctuation
SARS-CoV-2	Severe Acute Respiratory Syndrome-Coronavirus-2
SMILES	Simplified molecular input line entry system



1. Introduction

The SARS-CoV-2 virus has been identified as the causal agent of the Coronavirus disease (COVID-19), swiftly spreading worldwide and evolving into a global pandemic in 2020 (Harrison, Lin, & Wang, 2020; Eslami & Jalili, 2020; Chitra et al., 2022). In terms of transmissibility, it has considerably eclipsed SARS and MERS in the number of afflicted persons and the large-scale geographic span of epidemic locations (Hu, Guo, Zhou, & Shi, 2021).

As of August 31, 2022, the COVID-19 pandemic has led to over 599 million cases and 6.4 million fatalities globally ([Weekly Epidemiological Update on COVID-19 – August 31, 2022](#)). The congruent efforts of researchers have led to the development of vaccines to protect against emanant SARS-CoV-2 strains. Several vaccinations have been licensed for use in adult, adolescent, and older children's populations, but no vaccine has been approved for newborns and children under five ([Bonanni et al., 2021](#); [Malcangi et al., 2022](#)). Once the vast majority of the world's vaccine-eligible population has been immunized, the younger, currently ineligible population is expected to be at greater risk of infection ([Mahaboob Ali, Bugarcic, Naumovski, & Ghildyal, 2022](#)). The ability to manage SARS-CoV-2 infections in the future depends on the availability and accessibility of competent COVID-19 medicines.

Despite developing and implementing various vaccinations, no viable therapeutic drugs are available to prevent or treat the disease. The availability of safe and effective treatments would significantly improve our capacity to control SARS-CoV-2 infections. Some drugs such as remdesivir, favipiravir, chloroquine, hydroxychloroquine, and interferons have been recently repurposed due to their established inhibitory potentials against SARS-CoV-2 ([Awadasseid, Wu, Tanaka, & Zhang, 2021](#); [Han, Wang, Ren, Wei, & Li, 2021](#); [Kannan et al., 2022](#)). The world is now keen on reintroducing the hoary rituals to the general population for treating the disease. There is a critical need to systematically evaluate herbal formulations against SARS-CoV-2 ([Khanna et al., 2021](#)). Even though several therapeutic studies are underway throughout the world, traditional medicine has the potential to combat COVID-19. In Siddha's medical literature, epidemics, and pandemics known as Kollai Noigal is described and treated effectively using herbal formulations ([Mathukumar, Sindhuja, Sivapriya, & Birundadevi, 2022](#)).

Ayurveda is one of the primordial holistic systems of medicine that uses plant extracts as a key constituent in its formulations. Several studies have investigated the possible use of natural compounds, such as ayurvedic formulations, which are already extensively used in India to treat diseases ([Ayatollahi et al., 2021](#)). The extensive usage of Ayurveda as alternative medicine offers an appealing option for developing effective COVID-19 therapies ([Singh et al., 2018](#); [Steel, Wardle, & Lloyd, 2020](#)). The present study investigates the efficacy of *Glycyrrhiza glabra* as a therapeutic agent for combatting COVID-19.

Liquorice, scientifically named *Glycyrrhiza glabra* (referred to in Tamil as "Athimadhuram"), is widely used as a traditional medicine in India for multiple therapeutic activities such as cough, jaundice, polydipsia, peptic

ulcer, burning micturition. It is an authoritative natural sweetener, 50–170 times sweeter than sucrose (Mukhopadhyay & Panja, 2008; Prabhu, Vijayakumar, Yabesh, Prakashbabu, & Murugan, 2021). The roots contain several bioactive chemical compounds, including Glycyrrhizin (~16%) and sugar constituents (~18%) as primary ingredients. Many scientific studies reported *Glycyrrhiza glabra* possesses significant therapeutic properties in regulating cortisol action, testosterone synthesis reduction, exerting estrogen-like activity, and reducing body fat (Armanini, Fiore, Mattarello, Bielenberg, & Palermo, 2002; Hasan, Ara, Mondal, & Kabir, 2021; Minnetti et al., 2022). Pharmacological studies exhibit the medicinal plant's antioxidant, anti-tumor, antibacterial, and anti-HIV properties. Recent literature identified strong evidence of liquorice's therapeutic effects against COVID-19 (Koyuncu et al., 2021). Liquiritin, one of the liquorice-derived flavone compounds, has displayed preventive action via type I interferon simulation. Glycyrrhetic acid and Glycyrrhizin inhibit the synthesis of inflammatory mediators and factors by blocking the ACE 2 binding to the spike protein of the virus, infusing antibacterial and antiviral effects (Sinha, Prasad, Islam, Chaudhary et al., 2021). The Ministry of AYUSH (Ayurveda, Yoga and Naturopathy, Unani, Siddha, and Homeopathy), a ministry of the Government of India, issued Siddha advisory guidelines for the practitioners to defend against COVID-19 by improving immunity through medications. Athimadhura Chooranam is listed as a viable Antiviral Siddha herb, with a prescribed 1 gm BD. The antiviral activity of the formulations and drugs is not established or claimed to have treatment efficacy against COVID-19. But many studies lauded the druggability of *Glycyrrhiza glabra* as an expedient medication for COVID-19. This study proposes the novel interactions of the phytoconstituents with the targets for *Glycyrrhiza glabra* through *in silico* analysis. The network pharmacology approach delivers the associations between the compounds–genes–diseases, revealing the targets' regulatory mechanisms. The systematic workflow of the proposed work is represented in Fig. 1.



2. Materials and methods

2.1 Mining of phytoconstituents and its target

The phytoconstituents of *Glycyrrhiza glabra* were retrieved from the Chemical Entities of Biological Interest (ChEBI) database (<https://www.ebi.ac.uk/chebi/>). Each compound's simplified molecular input line entry

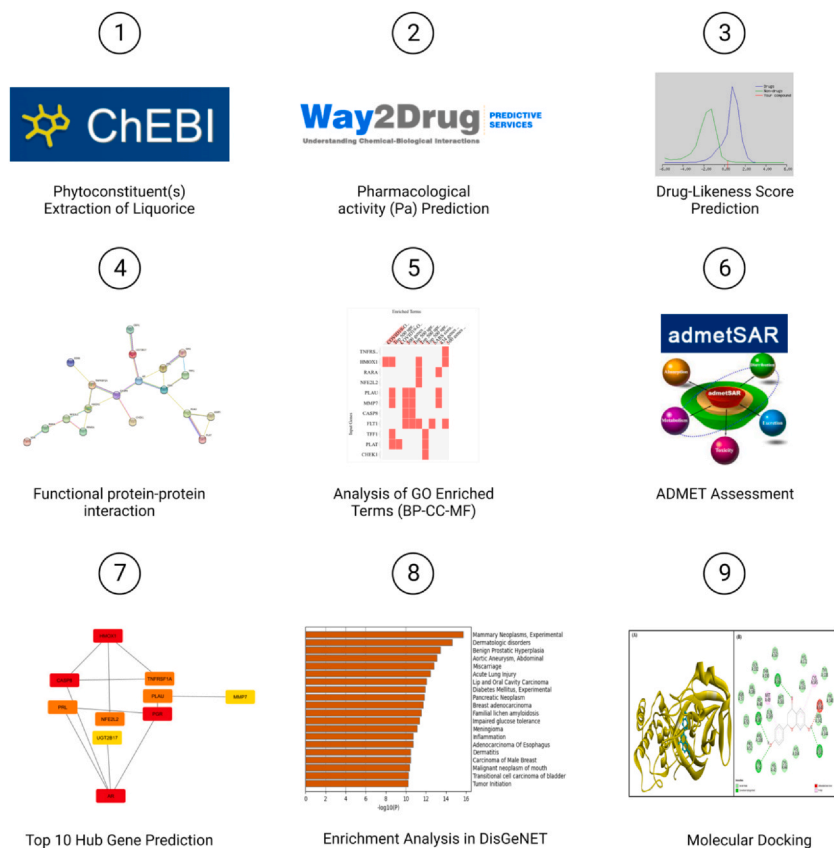


Fig. 1 The schematic representation shows the workflow of the network pharmacology approach.

system (SMILES) is inputted into the tool, identifying the genes based on mRNA expressions. In total, 59 phytoconstituents were fetched from the database, and each target was identified using the DIGEP-Pred tool (<http://www.way2drug.com/ge/>) for the proteins delivering the pharmacological activity (Pa) > 0.7.

2.2 Enrichment and network analysis

The protein-protein interaction, enrichment analysis, and gene ontology enrichment analysis are performed using the STRING (<https://string-db.org/>) and EnrichR tools (<https://maayanlab.cloud/Enrichr/>). The Cytoscape interface (<https://cytoscape.org/>) is used to construct the functional gene network. The go enrichment of molecular function, cellular component, and

biological process is performed using the KEGG pathway database synched with EnrichR. The disease association is calculated between COVID-19 and the genes using *p*-value significance on the literature mining results.

2.3 Druglikeness and ADMET profiling

Druglikeness is an assessment to qualitatively identify the chance for a molecule or a substance to become a “druglike” oral compound based on bioavailability. The score of each phytoconstituents is calculated to find the drug-likeness for identifying the probable effective individual. Lipinski’s rule of five is the protocol followed to extract the information using the MolSoft web server. ADMET parameters such as blood-brain barrier (BBB) permeability, P-glycoprotein inhibition, human intestinal absorption, hepatotoxicity, and human oral bioavailability were predicted for each component using admetSAR2.0 (<http://lmmd.ecust.edu.cn/admetSar2/>).

2.4 Molecular docking

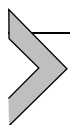
The Main Protease Proteins (MPP) play a crucial role in SARS-Cov-2 replication and are considered one of the potential drug targets (Anand, Ziebuhr, Wadhwani, Mesters, & Hilgenfeld, 2003; Zumla, Chan, Azhar, Hui, & Yuen, 2016). The crystal structure of COVID-19 main protease (PDB ID: 6LU7) was obtained from the RCSB-PDB (<https://www.rcsb.org/>). PyMOL software removed the water molecules and other ligand compounds attached to the protein structure before initiating the docking process. The 3D structure of the Liquiritigenin was retrieved from the PubChem Database in SDF format. The Open Babel software was used to convert the ligand file from SDF to PDB file format, further converted into. pdbqt file format using Autodock Vina 1.5.6. The center point parameters for the grid box generation were set to X: -11.728, Y: 13.798, and Z: 69.229, while the dimensions were X: 40, Y: 48, and Z: 48. BIOVIA Discovery Studio was used to visualize the interactions between the docked protein–ligand complex, and the docking conformations were analyzed.

2.5 Molecular dynamics simulation

The conformations of the MPP protein–ligand complex obtained from molecular docking calculations were further utilized in the simulation studies. The MD simulations were run for all the atoms in the MPP protein prior to and after the binding with the liquiritigenin compound. The molecular dynamics simulation studies used the GROMACS 2022.1

package and the GROMOS 54A7 force field. The ligand topology and other parameter files were generated using the PRODRG server (<http://davapc1.bioch.dundee.ac.uk/cgi-bin/prodrg>) and then were merged with the protein topology to form the simulation complexes. The structures were neutralized and then solvated into a cubical box using the SPC water model. To eliminate the sterical hindrances, the protein, and the protein–ligand complex systems were subjected to energy minimization for 5000 steps using the steepest descent approach followed by a conjugate gradient algorithm.

Furthermore, the minimized systems were subjected to position restrained ensembles conditions (NVT and NPT) at 300 K for 50,000 ps for equilibration. Berendsen's weak coupling and the Parrinello-Rahman approach (Martoňák, Laio, & Parrinello, 2003) were used to keep the system temperature and pressure at 300 K and 1 bar, respectively. The electrostatic interactions were calculated using Fast Particle-Mesh Ewald electrostatics (PME) and using the LINCS (Pearlman et al., 1995) algorithm, a long-range production MD run for both WT and protein–ligand at 100 ns. Using GROMACS utility tools, the *g_rmsf*, *g_rmsd*, *g_gyrate*, *g_sasa*, and *g_hbond*, the MD trajectories were examined to understand the structural and conformational changes (Welch, Arévalo, Turner, & Gómez, 2005).



3. Results

3.1 Phytoconstituents and their target

In total, 59 phytoconstituents were identified by the ChEBI database. The threshold of $Pa > 0.7$ scrutinizes the list and reduces it to 33 compounds. Liquiritigenin and 4', 7-dihydroxy flavanone are predicted to have a higher level of interaction with multiple proteins to a maximum of 6. Interestingly, these two compounds interact with the same gene set: one down-regulated (*NFE2L2*) and five up-regulated (*HMOX1*, *NFE2L2*, *PLAT*, *PLAU*, and *PGR*) genes. Further, among these six genes, *HMOX1*, *PLAU*, and *PGR* are commonly present in the top 10 ranked genes predicted by CytoHubba. *PLAU*, *MMP7*, *PLAT*, and *NFE2L2* are predicted to be highly targeted proteins by 10, 9, 9, and 8 phytoconstituents, respectively. Eighty-two targets interacted with 59 phytochemicals; only 22 were unique. The protein CD86 shows the highest pharmacological activity, scoring 0.937 for the component isoliquiritin.

3.2 Gene-set enrichment analysis and network analysis

The Gene Ontology (GO) enrichment analysis for the target proteins in BP, CC, and MF is examined using the EnrichR web server. Tables 1, 2, and 3 represent the top 10 enriched GO terms concerning the p -value, adjusted p -value, and odds ratio of BP, MF, and CC, respectively. The ranking of GO terms is calculated based on the combined score. The target protein interaction with COVID-19 is computed from the literature and is depicted in Fig. 2. The STRING online tool builds the PPI network encompassing all the proteins. Each edge in the network is assigned a score called the edge weight to compute the interaction confidence. This score shows the estimated likelihood that a specific interaction is biologically significant. PPIs with confidence scores of ≥ 0.4 were chosen to ensure interaction quality and reduce false-positive outcomes. The PPI network for proteins is given in Fig. 3 and consists of 19 nodes and 23 edges with an average node degree of 2.09; three isolated nodes (*KRT1*, *FLT1*, and *ALPPL2*) were excluded from the network.

Cytoscape is used to analyze and visualize the STRING data to investigate the probable interactions of these genes. The Maximal Clique Centrality topology analysis method ranks the network's top genes. The following genes, *AR*, *PGR*, *CASP8*, and *HMOX1*, are ranked top, with a score of 4 marked in red in Fig. 4. Similarly, *NFE2L2*, *PLAU*, *PRL*, and *TNFRSF1A* scored 3, and *PPARA* and *MMP7* are ranked 2, colored saffron and yellow, respectively. These genes are strongly associated with the immunity boost against COVID-19 (Khanal, Duyu et al., 2020). The enrichment analysis of disease terms identified from the DisGeNET database is depicted in Fig. 5, and the network of enriched terms clustered by the corresponding ID is visualized in Fig. 6.

3.3 Druglikeness and ADMET profiling

Forty compounds exhibit positive drug-likeness scores among 59 phyto-constituents. The highest drug-likeness score is attained by glyasperin C (1.15), followed by glyasperin D (1.14), (S)-reticuline (1.13), and dihydrolicoisoflavone A (1.11) scored >1 . The ADMET assessment revealed six compounds predicted to have positive scores for all five parameters. The compounds are listed—S-(–)-7,8-Didehydrocorydalmine, glyasperin F, isoliquiritigenin, isoliquiritin, glycyarpan, liquiritigenin, and edulol (ordered by the drug-likeness score—high to low).

Table 1 Biological process.

Index	Name	P-value	Adjusted p-value	Odds ratio	Combined score
1	Positive regulation of T-helper 2 cell differentiation (GO:0045630)	0.00001728	0.0009397	499.35	5475.89
2	Death-inducing signaling complex assembly (GO:0071550)	0.00002417	0.0009800	399.46	4246.35
3	Fibrinolysis (GO:0042730)	5.211e-7	0.0001373	262.71	3800.73
4	Regulation of T-helper 2 cell differentiation (GO:0045628)	0.00003221	0.001213	332.87	3442.91
5	Plasminogen activation (GO:0031639)	0.00004139	0.001454	285.30	2879.41
6	Growth hormone receptor signaling pathway via JAK-STAT (GO:0060397)	0.0001043	0.002617	166.38	1525.49
7	Positive regulation of T-helper cell differentiation (GO:0045624)	0.0001043	0.002617	166.38	1525.49
8	Positive regulation of type 2 immune response (GO:0002830)	0.0001043	0.002617	166.38	1525.49
9	Cellular response to estrogen stimulus (GO:0071391)	0.0001202	0.002640	153.58	1386.20
10	Steroid hormone mediated signaling pathway (GO:0043401)	0.0001202	0.002640	153.58	1386.20

Table 2 Molecular function.

Index	Name	P-value	Adjusted p-value	Odds ratio	Combined score
1	RNA polymerase II general transcription initiation factor binding (GO:0001091)	0.005488	0.02077	237.79	1237.70
2	Tumor necrosis factor binding (GO:0043120)	0.005488	0.02077	237.79	1237.70
3	Carbonyl reductase (NADPH) activity (GO:0004090)	0.005488	0.02077	237.79	1237.70
4	Transcription coactivator binding (GO:0001223)	0.0002168	0.007882	110.89	935.50
5	Retinoic acid binding (GO:0001972)	0.0002633	0.007882	99.79	822.50
6	Histone threonine kinase activity (GO:0035184)	0.007676	0.02449	158.51	771.89
7	Vascular endothelial growth factor-activated receptor activity (GO:0005021)	0.007676	0.02449	158.51	771.89
8	Protein kinase B binding (GO:0043422)	0.008768	0.02540	135.86	643.51
9	Bile acid binding (GO:0032052)	0.009858	0.02540	118.87	549.11
10	Tumor necrosis factor-activated receptor activity (GO:0005031)	0.009858	0.02540	118.87	549.11

Table 3 Cellular component.

Index	Name	P-value	Adjusted p-value	Odds ratio	Combined score
1	CD95 death-inducing signaling complex (GO:0031265)	0.005488	0.06313	237.79	1237.70
2	Endosome lumen (GO:0031904)	0.0003694	0.01330	83.14	657.12
3	Death-inducing signaling complex (GO:0031264)	0.008768	0.06313	135.86	643.51
4	Condensed nuclear chromosome (GO:0000794)	0.02178	0.1307	50.02	191.42
5	Cornified envelope (GO:0001533)	0.04627	0.1775	22.60	69.47
6	Condensed chromosome (GO:0000793)	0.05778	0.1775	17.90	51.04
7	Extracellular membrane-bounded organelle (GO:0065010)	0.05985	0.1775	17.25	48.57
8	Extracellular vesicle (GO:1903561)	0.06296	0.1775	16.35	45.22
9	Cytoskeleton (GO:0005856)	0.003815	0.06313	7.23	40.24
10	Collagen-containing extracellular matrix (GO:0062023)	0.008015	0.06313	8.21	39.62

Top 500 upregulated genes for SARS-CoV-2 in human colon organoid from GSE148696

500 genes up-regulated by SARS-CoV-2 in human Lung Organoid cells at 24 hpi from GSE148697

Top 500 upregulated genes for SARS-CoV-2 infection in human lung organoids from GSE148697

Top 500 upregulated genes in mouse D2 cardiomyocytes with SARS-CoV-2 infection from GEO GSE162113

COVID19-Orf3a protein host PPI from Krogan

Top 500 upregulated genes in human nasal epithelial cells with SARS-CoV-2 infection (Wild Type, 24 hpi) from GEO GSE148697

434 genes down-regulated by SARS-CoV-2 in ferret trachea from GSE147507

500 genes up-regulated by SARS-CoV-2 in human pancreatic organoids from GSE151803

500 top upregulated genes from SARS-CoV-2 infection at 72 HPI from GSE157852

500 genes down-regulated by SARS-CoV-2 382-deletion mutant in human Nasal Epithelial Cells cells at 24 hpi from GSE148697

Fig. 2 Representation of target interaction with COVID-19 from the literature search.

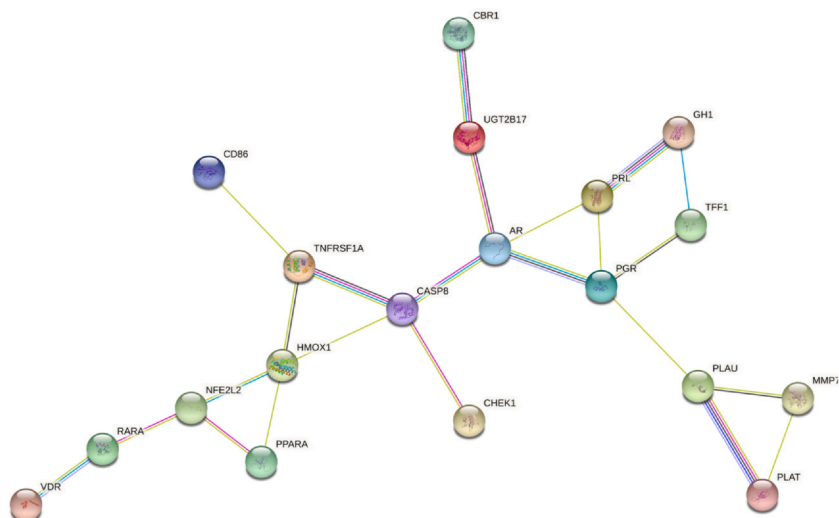


Fig. 3 Protein-protein interaction network of the target proteins using the STRING tool.

3.4 Molecular docking

The MPP is responsible for cleavage the viral polyprotein at eleven distinct locations, resulting in the formation of diverse Nsps needed for viral replication. MPP directly mediates Nsps maturation, which is required in the virus's life cycle. The involvement of the MPP in the replication process makes it an appealing target for COVID-19 therapeutic development. The AutoDock Tools 1.5.6 were used to perform the Docking of MPP with the liquiritigenin phytochemical compound. The liquiritigenin,

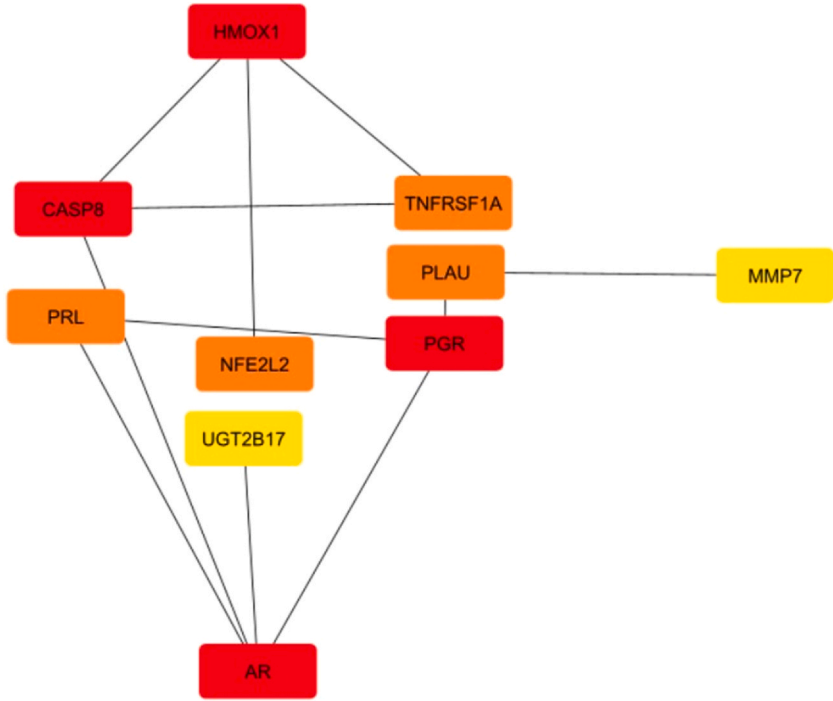


Fig. 4 The top 10 genes predicted using the Cytohubba plugin. The darker red hue represents a higher rating among the genes.

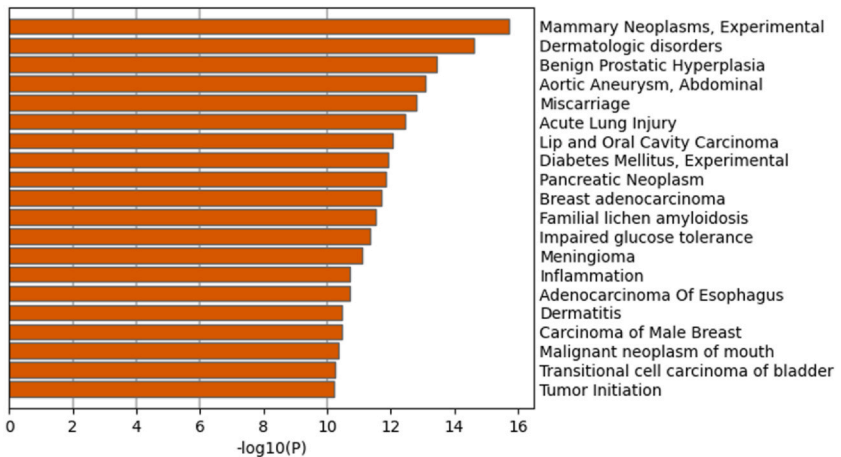


Fig. 5 Summary of enrichment analysis using DisGeNET.

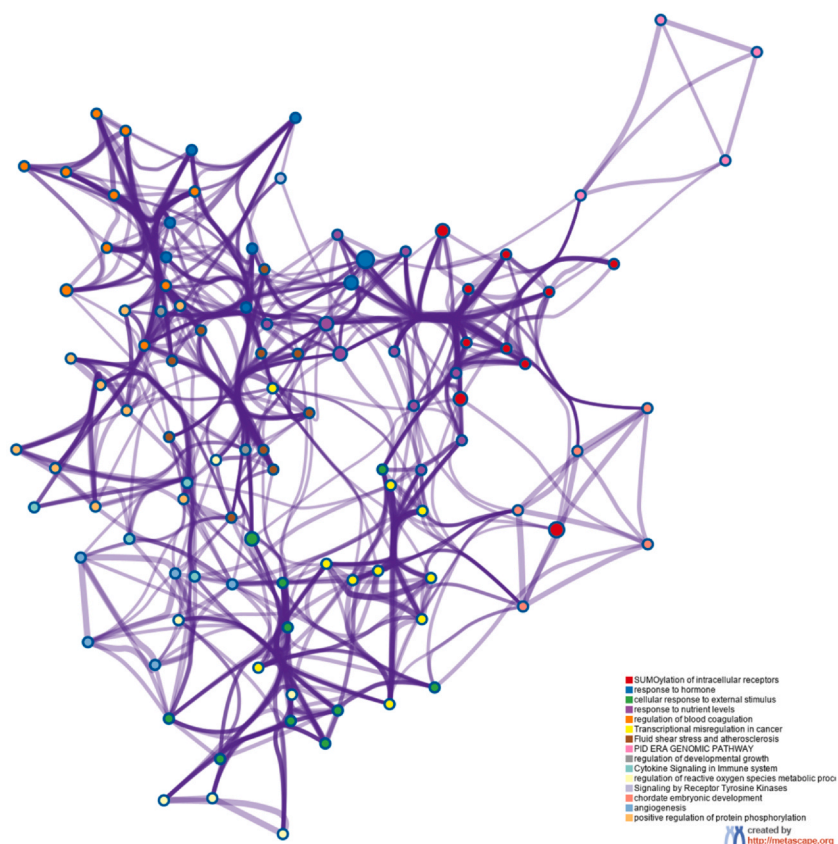


Fig. 6 Representation of network for enriched terms where each cluster-ID is differentiated by color, nodes that share the same cluster-ID are typically closer to each other.

when docked with the main protease protein, showed a binding affinity of -7.7 kcal/mol, and the interactions between the active sites of MPP and liquiritigenin were observed to be highly coherent. The MPP–liquiritigenin docked complex resulted in four H-bonds with Y54, L141, E166, and D187, two pi-alkyl interactions with M49 and C145, and one unfavorable donor–donor interaction was observed at G143 (Fig. 7).

3.5 Molecular dynamics simulation

The goal of the long-range MD simulations is to learn more about the conformational stability of the docked protein–ligand complexes in comparison to the wild-type protein. The root-mean-square deviation (RMSD)

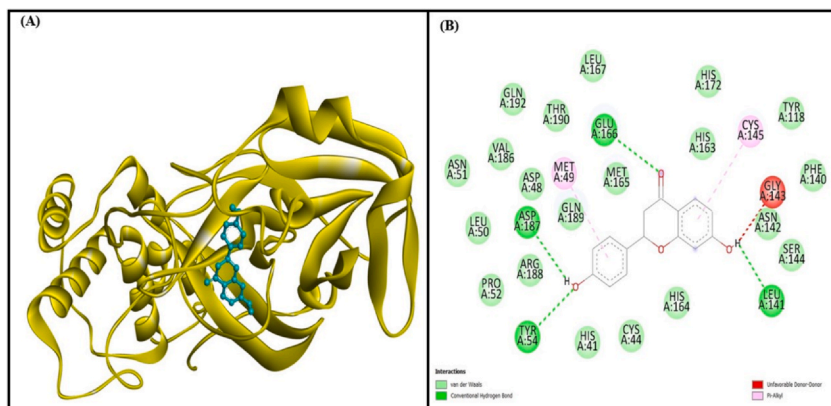


Fig. 7 Representation of interactions between the liquiritigenin and main protease protein (MPP). The ligand interaction diagram represents the 2D ligand interactions from Discovery studio. The green, red and purple residue interactions represent the hydrogen bonds, and unfavorable donor-donor and pi-alkyl interactions respectively.

is conventionally used to gain insight into the structural endurance of the proteins. The RMSD of MPP protein was calculated in free and complex states to examine its structural dynamics. The wild-type MPP protein and the complex had average RMSDs of 0.9 and 0.23 nm, respectively (Fig. 8A). The fluctuation of each residue was assessed as root-mean-square fluctuation (RMSF) to estimate the residual vibrations in the free and ligand-bound MPP protein. Fluctuations were seen randomly at the N-terminal and C-terminal regions in MPP protein in both wild-type and ligand-bound states. The protein residues in the ligand-bound complex showed little variation in the 0.2 nm range (Fig. 8B). The fluctuation in the wild-type protein, when compared with the bound complex, showed higher fluctuations in the range of 0.48–0.78 nm. The lesser number of fluctuating residues again indicates stable protein–ligand systems in MD simulation.

Another critical metric is the radius of gyration (Rg), which is connected with the compactness and folding behavior of the protein within a biological system. A high Rg value indicates that the amino acid residues in a protein are crudely packed. The average Rg values for MPP wild-type and ligand-bound systems were 2.32 nm and 2.25 nm, respectively (Fig. 8C). The ligand-bound complex showed stable Rg throughout the simulation study. SASA refers to the surface area of proteins attainable for interaction within the encompassed water. It's a basic parameter that gives insight into the protein folding dynamics within a solvated environment.

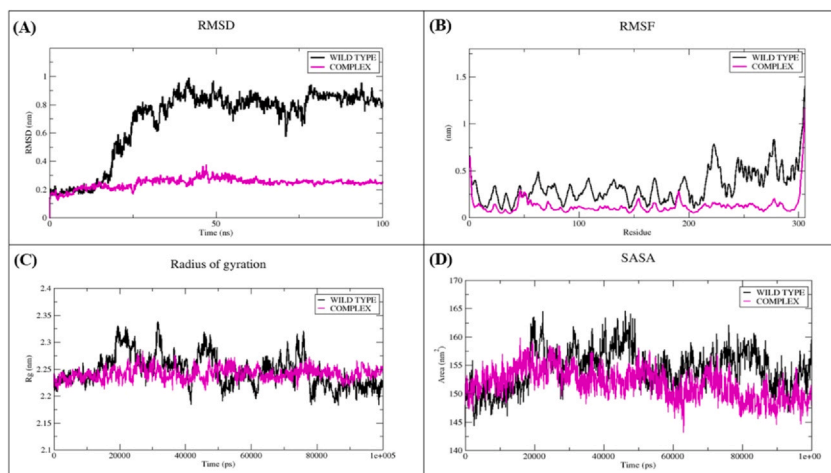


Fig. 8 Representation of Molecular dynamic simulation for SARS-CoV-2 MPP protein and protein–ligand complexes during 100 ns simulation (A) RMSD of MPP protein and MPP–liquiritigenin complex during 100 ns MD simulation (B) RMSF values of MPP protein and MPP–liquiritigenin complex during 100 ns MD simulation (C) Rg values of MPP protein and MPP–liquiritigenin complex during 100 ns MD simulation. (D) SASA values of MPP protein and MPP–liquiritigenin complex during 100 ns MD simulation. The unbound protein system is depicted in black color. The parameters for the MPP–liquiritigenin complex are represented in magenta color.

The SASA values were 157.5 nm^2 and 164 nm^2 for wild-type and ligand-bound structures, respectively (Fig. 8D). SASA results show that the binding of MPP protein with the liquiritigenin makes it more stable and compact than the MPP unbound structure. Intramolecular hydrogen bonding is an important factor that plays a key role in determining its structure and conformation. The number of intramolecular hydrogen bonds was computed to evaluate the stability of MPP protein in wild-type conformation. The wild-type MPP protein showed an average of 225 hydrogen bonds (Fig. 9A).

Further, the hydrogen bonds between the protein and the ligand were evaluated to understand the interaction pattern during the protein–ligand binding. The number of hydrogen bonds formed between the protein and the inhibitor was assessed to get insights into the binding stability between MPP protein and liquiritigenin. An average of 2–3 H-bonds formed between the protein–ligand complex (Fig. 9B); however, a significant H-bond loss can be seen after 80 ns.

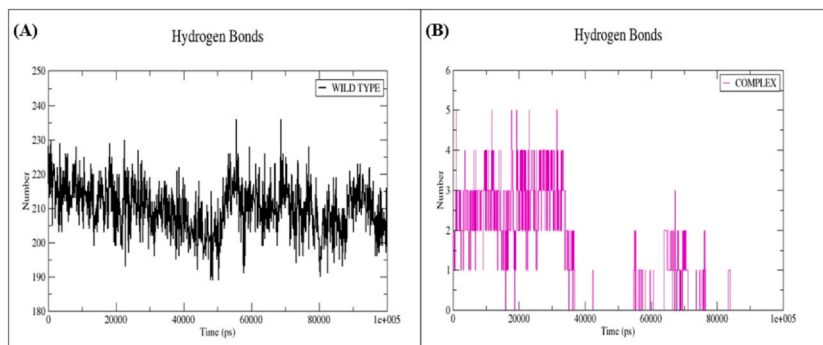


Fig. 9 Representation of hydrogen bond analyses for MPP protein and protein-ligand complexes during 100 ns simulation. (A) Number of hydrogen bonds in the unbound MPP protein. (B) The hydrogen bonds between MPP protein and the ligand Liquiritigenin. Unbound MPP protein is depicted in black color. Parameters for the MPP–liquiritigenin complex are represented in magenta color.

4. Discussion

The demand for a novel, effective therapeutic drug to inhibit SARS-CoV-2 is surging globally. The impediment of the pandemic outbreak can only be controlled with authoritative medication. The elderly and individuals with comorbidity are highly vulnerable to the transmission of SARS-CoV-2 disease. The increase in mortality rate and the reduction in survival rate is directly proportional to the physical health condition of the individuals (Hasson et al., 2022; Khademi, Moayedi, & Golitaleb, 2021). The major challenge in the treatment protocol is improving the declining health of COVID-19 patients with comorbidities. The current medication or the clinical condition could hamper the efficacy of the COVID-19 drug or worsen physical well-being. Traditional medicines are the products of natural substances, which are widely used therapeutics to treat various clinical conditions. The knowledge of ancient medicinal practices still delivers unprecedented effects on curing complex diseases (Nogales et al., 2021).

Recently, many studies have been conducted worldwide on varieties of traditional medical techniques. Kalmegh (*Andrographis paniculata*), an ayurvedic herb, delivers immunoprotective potential against respiratory viral diseases, including SARS-CoV-2 (Hiremath et al., 2021; Mishra, Shaik, Sinha, & Shah, 2021; Wanaratna et al., 2021). This study investigated the herbal activity of respiratory infections using a network pharmacology approach (Banerjee et al., 2021). In a similar study, the Ministry

of AYUSH recommended that herbal tea containing ayurvedic phytoconstituents be analyzed and find gene modulations and novel signaling pathways that boost immunity (Khanal, Patil, Chand, & Naaz, 2020). The decoction includes the components such as *Ocimum tenuiflorum*, *Piper nigrum*, *Cinnamomum verum*, *Vitis vinifera*, and *Zingiber officinale*, a natural immune booster. An *in silico* investigation of the medicinal herb *Tinospora cordifolia* (giloy) is performed to identify its biological functions. The molecular docking and simulation revealed the SARS-CoV-2 inhibition properties of the target compound (Chowdhury, 2021; Murugesan et al., 2021).

Mucormycosis, a life-threatening disease, occurs when the individual's immune system is heavily compromised under various circumstances, such as COVID-19. Covid Associated Mucormycosis (CAM) management strategies with the phytocompounds such as turmeric and neem are proposed in this network pharmacological study. The outcome revealed Quercetin, an active phytocompound, effectively works against Mucormycosis (Datta, Sarkar, Sen, & Sen, 2022; Malabadi, Kolkar, Meti, & Chalannavar, 2021; Sekar, Ramasamy, & Ravikumar, 2022). In a pharmacoinformatics study, the bioactive components of *Glycyrrhiza glabra* are examined for consideration as a potential inhibitor of SARS-CoV-2 glycoprotein. This study concluded that glyasperin A and glycyrrhizic acid as potential compounds from liquorice as a defendant of COVID-19 (Maddah et al., 2021; Sinha, Prasad, Islam, Gurav et al., 2021). The same phytoconstituents are identified in the present study as potential candidates for the target disease.

The AYUSH-recommended Siddha medicine, Athimadthuram Chooranam containing *Glycyrrhiza glabra*, is studied for its immune-boosting, antiviral properties against SARS-CoV-2. The multiple phytoconstituents identified from the ChEBI database are analyzed using a network pharmacology approach. The enrichment analysis and protein-protein interaction between the multitarget and multi-components are performed with bioinformatic methods. The lead hit molecules were identified by calculating the drug-likeness score of each component based on Lipinski's Rule of Five. The substance of interest is a prescribed intake formulation. Therefore, human intestinal absorption and other ADMET properties are calculated for the viable components scoring the pharmacological activity (Pa) > 0.7 . Among all, glyasperin C attained a higher drug-likeness score of 1.15. Liquiritigenin revealed better significance than other active bio compounds with better ADMET and drug-likeness scores.

Molecular docking is a sophisticated computational approach for predicting the binding ability of a target protein to small molecules via hydrogen bonds and hydrophobic interactions. The selected natural compound liquiritigenin was docked onto the binding site of the MPP protein. The docking results showed that the natural compound is efficiently involved in hydrogen bonding and hydrophobic interactions with the active site residues of the MPP protein. The dynamic structural and conformational variations in the MPP protein–ligand complex were determined using molecular dynamics simulations. The significant difference between the RMSD values of MPP bound and unbound structures reveals that the protein backbone stabilizes when complexed with the liquiritigenin compound. According to the RMSF data, the ligand-bound complex exhibits fewer fluctuations than the wild-type MPP protein indicating a stable protein–ligand complex. Rg analysis of ligand-bound MPP showed a lesser range of Rg values and is throughout the simulation study. SASA and H-bond analysis studies show that the liquiritigenin binding to the MPP protein has formed a stable complex. Further detailed studies on liquiritigenin will unveil novel mechanisms and insights to effectively stand as a potential therapeutic against SARS-CoV-2.



5. Conclusion

This study proposes an in silico network pharmacology study on *Glycyrrhiza glabra*, an active component of Athimadhura Chooranam. The Ministry of AYUSH recommends this Siddha medicine as an effective antiviral herbal medication against SARS-CoV-2. The bioinformatic analysis identified the immune-boosting, multi-faceted therapeutic effect on the selected phytochemical of interest against the target. Liquiritigenin, a natural bioactive substance in *Glycyrrhiza glabra*, displayed phenomenal effects during drug-likeness assessment and ADMET evaluation. This compound could act as a potential inhibitor of SARS-CoV-2. Molecular docking studies are gaining better attention and are widely used as a powerful approach in structural molecular biology for structure-based drug design through computer-assisted models. This study will be developed by fusing *in silico* drug development phase with currently screened phytoconstituents of *Glycyrrhiza glabra*. The outcome of the proposed network pharmacology approach envisages building a computational framework predicting the bioactive phytoconstituents and serving as an effective

therapeutic against SARS-CoV-2. Furthermore, building artificial intelligence-based ranking phytoconstituents algorithms can further enhance the predictions.

CRediT authorship contribution statement

Author contributions KS, AK, RPV, PS, MSSD, RS and GPDC were involved in the study design. KS, RPV, PS, MSSD, RS and GPDC acquired, analyzed and interpreted the results. GPDC, MSSD and RS supervised the entire study. KS and RPV drafted the manuscript. All authors edited and approved the submitted version of the article.

Data availability statement

The data are available with the corresponding author GPDC.

Declaration of competing interest

The authors declare that they have no known competing financial interests.

Appendix A. Supporting information

Supplementary data associated with this article can be found in the online version at <http://doi.org/10.1016/bs.apcsb.2023.04.003>.

References

- Anand, K., Ziebuhr, J., Wadhwani, P., Mesters, J. R., & Hilgenfeld, R. (2003). Coronavirus main proteinase (3CLpro) structure: Basis for design of anti-SARS drugs. *Science (New York, N. Y.)*, 300(5626), 1763–1767. <https://doi.org/10.1126/science.1085658>
- Armanini, D., Fiore, C., Mattarello, M. J., Bielenberg, J., & Palermo, M. (2002). History of the endocrine effects of licorice. *Experimental and Clinical Endocrinology & Diabetes*, 110(06), 257–261.
- Awadasseid, A., Wu, Y., Tanaka, Y., & Zhang, W. (2021). Effective drugs used to combat SARS-CoV-2 infection and the current status of vaccines. *Biomedicine & Pharmacotherapy*, 137, 111330.
- Ayatollahi, S. A., Sharifi-Rad, J., Tsouh Fokou, P. V., Mahady, G. B., Ansar Rasul Suleria, H., Krishna Kapuganti, S., ... Cruz-Martins, N. (2021). Naturally occurring bioactives as antivirals: Emphasis on coronavirus infection. *Frontiers in Pharmacology*, 12, 575877. <https://doi.org/10.3389/fphar.2021.575877>
- Banerjee, S., Kar, A., Mukherjee, P. K., Haldar, P. K., Sharma, N., & Katiyar, C. K. (2021). Immunoprotective potential of ayurvedic herb Kalmegh (*Andrographis paniculata*) against respiratory viral infections—LC–MS/MS and network pharmacology analysis. *Phytochemical Analysis*, 32(4), 629–639.
- Bonanni, P., Angelillo, I. F., Villani, A., Biasci, P., Scotti, S., Russo, R., & Azzari, C. (2021). Maintain and increase vaccination coverage in children, adolescents, adults and elderly people: Let's avoid adding epidemics to the pandemic: Appeal from the Board of the Vaccination Calendar for Life in Italy: Maintain and increase coverage also by re-organizing vaccination services and reassuring the population. *Vaccine*, 39(8), 1187–1189.
- Chitra, S. M., Mallika, P., Anbu, N., Narayanababu, R., Sugunabai, A., David Paul Raj, R. S., & Premnath, D. (2022). An open clinical evaluation of selected Siddha regimen in expediting the management of COVID-19—A randomized controlled study. *Journal of Ayurveda and Integrative Medicine*, 13(1), 100397. <https://doi.org/10.1016/j.jaim.2021.01.002>

- Chowdhury, P. (2021). In silico investigation of phytoconstituents from Indian medicinal herb 'Tinospora cordifolia (giloy)' against SARS-CoV-2 (COVID-19) by molecular dynamics approach. *Journal of Biomolecular Structure and Dynamics*, 39(17), 6792–6809.
- Datta, S., Sarkar, I., Sen, G., & Sen, A. (2023). Neem and turmeric in the management of Covid Associated Mucormycosis (CAM) derived through network pharmacology. *Journal of Biomolecular Structure and Dynamics*, 41(8), 3281–3294.
- Eslami, H., & Jalili, M. (2020). The role of environmental factors to transmission of SARS-CoV-2 (COVID-19). *AMB Express*, 10(1), 92.
- Han, Y., Wang, Z., Ren, J., Wei, Z., & Li, J. (2021). Potential inhibitors for the novel coronavirus (SARS-CoV-2). *Briefings in Bioinformatics*, 22(2), 1225–1231.
- Harrison, A. G., Lin, T., & Wang, P. (2020). Mechanisms of SARS-CoV-2 transmission and pathogenesis. *Trends in Immunology*, 41(12), 1100–1115.
- Hasan, M. K., Ara, I., Mondal, M. S. A., & Kabir, Y. (2021). Phytochemistry, pharmacological activity, and potential health benefits of *Glycyrrhiza glabra*. *Heliyon*, 7(6), e07240.
- Hasson, R., Sallis, J. F., Coleman, N., Kaushal, N., Nocera, V. G., & Keith, N. (2022). COVID-19: Implications for physical activity, health disparities, and health equity. *American Journal of Lifestyle Medicine*, 16(4), 420–433.
- Hiremath, S., Kumar, H. D., Nandan, M., Mantesh, M., Shankarappa, K. S., Venkataravanappa, V., & Reddy, C. N. (2021). In silico docking analysis revealed the potential of phytochemicals present in *Phyllanthus amarus* and *Andrographis paniculata*, used in Ayurveda medicine in inhibiting SARS-CoV-2. *3 Biotech*, 11(2), 44.
- Hu, B., Guo, H., Zhou, P., & Shi, Z.-L. (2021). Characteristics of SARS-CoV-2 and COVID-19. *Nature Reviews. Microbiology*, 19(3), 141–154. <https://doi.org/10.1038/s41579-020-00459-7>
- Kannan, M., Sathiyarajeswaran, P., Sasikumar, D., Geetha, A., Mohanapriya, M., Vinod, N. P., ... Sivaraman, G. (2022). Safety and efficacy of a Siddha medicine fixed regimen for the treatment of asymptomatic and mild COVID-19 patients. *Journal of Ayurveda and Integrative Medicine*, 13(3), 100589. <https://doi.org/10.1016/j.jaim.2022.100589>
- Khademi, F., Moayedi, S., & Golitaleb, M. (2021). The COVID-19 pandemic and death anxiety in the elderly. *International Journal of Mental Health Nursing*, 30(1), 346.
- Khanal, P., Duyu, T., Patil, B. M., Dey, Y. N., Pasha, I., Wanjari, M., ... Maity, A. (2020). Network pharmacology of AYUSH recommended immune-boosting medicinal plants against COVID-19. *Journal of Ayurveda and integrative medicine*, 100374.
- Khanal, P., Patil, B. M., Chand, J., & Naaz, Y. (2020). Anthraquinone derivatives as an immune booster and their therapeutic option against COVID-19. *Natural Products and Bioprospecting*, 10(5), 325–335.
- Khanna, K., Kohli, S. K., Kaur, R., Bhardwaj, A., Bhardwaj, V., Ohri, P., ... Ahmad, P. (2021). Herbal immune-boosters: Substantial warriors of pandemic Covid-19 battle. *Phytomedicine: International Journal of Phytotherapy and Phytopharmacology*, 85, 153361. <https://doi.org/10.1016/j.phymed.2020.153361>
- Koyuncu, İ., Durgun, M., Yorulmaz, N., Toprak, S., Gonel, A., Bayraktar, N., & Caglayan, M. (2021). Molecular docking demonstration of the liquorice chemical molecules on the protease and ACE2 of COVID-19 virus. *Current Enzyme Inhibition*, 17(2), 98–110.
- Maddah, M., Bahramsoltani, R., Yekta, N. H., Rahimi, R., Aliabadi, R., & Pourfath, M. (2021). Proposing high-affinity inhibitors from *Glycyrrhiza glabra* L. against SARS-CoV-2 infection: Virtual screening and computational analysis. *New Journal of Chemistry*, 45(35), 15977–15995.
- Mahaboob Ali, A. A., Bugarcic, A., Naumovski, N., & Ghildyal, R. (2022). Ayurvedic formulations: Potential COVID-19 therapeutics? *Phytomedicine Plus*, 2(3), 100286. <https://doi.org/10.1016/j.phyplu.2022.100286>

- Malabadi, R. B., Kolkar, K. P., Meti, N. T., & Chalannavar, R. K. (2021). Outbreak of coronavirus (SARS-CoV-2) delta variant (B. 1.617. 2) and delta plus (AY. 1) with fungal infections, mucormycosis: Herbal medicine treatment. *International Journal of Research and Scientific Innovations*, 8(6), 59–70.
- Malcangi, G., Inchingolo, A. D., Inchingolo, A. M., Piras, F., Settanni, V., Garofoli, G., ... Dipalma, G. (2022). COVID-19 infection in children and infants: Current status on therapies and vaccines. *Children*, 9(2), 249.
- Martonoák, R., Laio, A., & Parrinello, M. (2003). Predicting crystal structures: The Parrinello-Rahman method revisited. *Physical Review Letters*, 90(7), 075503. <https://doi.org/10.1103/PhysRevLett.90.075503>
- Mathukumar, S., Sindhuja, T., Sivapriya, T., & Birundadevi, M. (2022). A review on selected South Indian regime of Tamil Nadu for the seasonal management of communicable diseases. *Journal of Pharmaceutical Research International*, 34, 7–18. <https://doi.org/10.9734/jpri/2022/v34i7B35467>
- Minnetti, M., De Alcubierre, D., Bonaventura, I., Pofi, R., Hasenmajer, V., Tarsitano, M. G., & Isidori, A. M. (2022). Effects of licorice on sex hormones and the reproductive system. *Nutrition (Burbank, Los Angeles County, Calif.)*, 103–104, 111727.
- Mishra, A., Shaik, H. A., Sinha, R. K., & Shah, B. R. (2021). Andrographolide: A herbal-chemosynthetic approach for enhancing immunity, combating viral infections, and its implication on human health. *Molecules (Basel, Switzerland)*, 26(22), 7036.
- Mukhopadhyay, M., & Panja, P. (2008). A novel process for extraction of natural sweetener from licorice (*Glycyrrhiza glabra*) roots. *Separation and Purification Technology*, 63(3), 539–545.
- Murugesan, S., Kottekad, S., Crasta, I., Sreevathsan, S., Usharani, D., Perumal, M. K., & Mudliar, S. N. (2021). Targeting COVID-19 (SARS-CoV-2) main protease through active phytochemicals of ayurvedic medicinal plants—*Emblica officinalis* (Amla), *Phyllanthus niruri* Linn. (Bhumi Amla) and *Tinospora cordifolia* (Giloy)—A molecular docking and simulation study. *Computers in Biology and Medicine*, 136, 104683.
- Nogales, C., Mamdouh, Z. M., List, M., Kiel, C., Casas, A. I., & Schmidt, H. H. (2022). Network pharmacology: Curing causal mechanisms instead of treating symptoms. *Trends in Pharmacological Sciences*, 43(2), 136–150.
- Pearlman, D. A., Case, D. A., Caldwell, J. W., Ross, W. S., Cheatham, T. E., DeBolt, S., ... Kollman, P. (1995). AMBER, a package of computer programs for applying molecular mechanics, normal mode analysis, molecular dynamics and free energy calculations to simulate the structural and energetic properties of molecules. *Computer Physics Communications*, 91(1), 1–41. [https://doi.org/10.1016/0010-4655\(95\)00041-D](https://doi.org/10.1016/0010-4655(95)00041-D)
- Prabhu, S., Vijayakumar, S., Yabesh, J. M., Prakashbabu, R., & Murugan, R. (2021). An ethnobotanical study of medicinal plants used in pachamalai hills of Tamil Nadu, India. *Journal of Herbal Medicine*, 25, 100400.
- Sekar, V., Ramasamy, G., & Ravikumar, C. (2022). In silico molecular docking for assessing anti-fungal competency of hydroxychavicol, a phenolic compound of betel leaf (*Piper betle* L.) against COVID-19 associated maiming mycotic infections. *Drug Development and Industrial Pharmacy*, 48(5), 169–188.
- Singh, H., Bhargava, S., Ganeshan, S., Kaur, R., Sethi, T., Sharma, M., ... Brahmachari, S. K. (2018). Big data analysis of traditional knowledge-based ayurveda medicine. *Progress in Preventive Medicine*, 3(5), e0020. <https://doi.org/10.1097/pp9.0000000000000020>
- Sinha, S. K., Prasad, S. K., Islam, M. A., Chaudhary, S. K., Singh, S., & Shakya, A. (2021). Potential leads from liquorice against SARS-CoV-2 main protease using molecular docking simulation studies. *Combinatorial Chemistry & High Throughput Screening*, 24(4), 591–597.
- Sinha, S. K., Prasad, S. K., Islam, M. A., Gurav, S. S., Patil, R. B., AlFaris, N. A., ... Shakya, A. (2021). Identification of bioactive compounds from *Glycyrrhiza glabra* as possible inhibitors of SARS-CoV-2 spike glycoprotein and non-structural protein-15: A pharmacoinformatics study. *Journal of Biomolecular Structure and Dynamics*, 39(13), 4686–4700.

- Steel, A., Wardle, J., & Lloyd, I. (2020). The potential contribution of traditional, complementary and integrative treatments in acute viral respiratory tract infections: Rapid reviews in response to the COVID-19 pandemic. *Advances in Integrative Medicine*, 7(4), 181–182. <https://doi.org/10.1016/j.aimed.2020.09.001>
- Wanaratna, K., Leethong, P., Inchai, N., Chueawiang, W., Sriraksa, P., Tabmee, A., & Sirinavin, S. (2021). Efficacy and safety of *Andrographis paniculata* extract in patients with mild COVID-19: A randomized controlled trial. *MedRxiv*.
- Weekly epidemiological update on COVID-19—August 31 2022. (n.d.). Retrieved September 1, 2022, from <https://www.who.int/publications/m/item/weekly-epidemiological-update-on-covid-19—31-august-2022>.
- Welch, K. T., Arévalo, S., Turner, J. F., & Gómez, R. (2005). An NMR and molecular modeling study of carbosilane-based dendrimers functionalized with phenolic groups or titanium complexes at the periphery. *Chemistry—A European Journal*, 11(4), 1217–1227.
- Zumla, A., Chan, J. F. W., Azhar, E. I., Hui, D. S. C., & Yuen, K.-Y. (2016). Coronaviruses—Drug discovery and therapeutic options. *Nature Reviews. Drug Discovery*, 15(5), 327–347. <https://doi.org/10.1038/nrd.2015.37>